



Quantum chemical analysis of harmful dye 3-[(4-anilinophenyl) diazenyl] benzenesulfonate, metanil yellow

Shreyas Parbat *

Department of Chemical Engineering, Indian Institute of Science, Bangalore, India

*Corresponding author E-mail: shreyasparbat2120@gmail.com

Abstract

In the present work, quantum chemical study of the harmful dye, metanil yellow is conducted. The optimized molecular geometry and harmonic vibrational frequencies of metanil yellow were calculated by DFT-B3LYP method with LANL2DZ basis set. The vibrational assignments were performed on the basis of the potential energy distribution (PED) of the vibrational modes. Infrared spectra and Bulk Raman spectra were also obtained and characteristic peaks for the title compound were studied. The nonlinear optical properties of the title compound were calculated and discussed. Dipole moment, polarizability and first-order hyperpolarizability of the title compound were reported in order to study nonlinear optical properties (NLO). HOMO-LUMO energy levels were also computed in order to get the bandgap energy. Global reactivity descriptors were calculated using the HOMO and LUMO to predict compound reactivity. UV-Vis spectrum of the title compound was calculated using TD-DFT method. The molecular orbital contributions were studied by density of states (DOSs). Mulliken atomic charges and atomic polar tensors (APT) on each atom were tabulated. A discussion of the vibrational energy of each mode is also presented in this article.

Keywords: DFT; Gaussian; Metanil Yellow; Nonlinear Optical Properties; Raman Spectra.

1. Introduction

Metanil yellow is an azo dye having yellow colour which is prepared by diazotization reaction and a coupling reaction. In recent times, metanil yellow have succeeded in achieving great attention due to its useful behaviour in the food industries. These kinds of dyes are used as food additives and food colorants. It is used as food adulterant in turmeric powder and various dals in India (Dhakal et al. 2016, Common food adulterants in India 2018). The title compound is used in coloring wool, detergent, paper, etc. It is a cheap colorant (Nath et al. 2016). Although, the title compound has gotten various wide applications in food industry, it belongs to the “nonpermitted” category of the food color (Ghosh et al. 2017). Even if metanil yellow has been used widely, it is proved that deliberate or indeliberate consumption can cause the damage to human body systems such as nervous system, digestive system, cardiovascular system as well as reproductive system (Ghosh et al. 2017). Experiments performed on several animals such as goat liver (Hazra et al. 2016) and rats (Sarkar et al. 2013) proved that the intake of the title compound is harmful. Consumption of this dye by any mean is quite risky for human health (Das et al. 1997). Hence, the proper quantum chemical study of this harmful dye is essential.

The structure of the metanil yellow was studied using Density Functional Theory (DFT) with B3LYP hybrid exchange correlation functional and LANL2DZ basis set. Potential Energy Distribution (PED) was studied by performing vibrational assignments. The B3LYP functional and LANL2DZ basis set of Density Functional Theory (DFT) helped us to investigate HOMO and LUMO molecular orbitals of metanil yellow. Non-Linear optic activity of metanil yellow was demonstrated by obtaining linear polarizability, hyperpolarizability and dipole moment. Atomic polar tensors (APT) and Mulliken atomic charge on each atom were obtained by Density Functional Theory method. UV-Vis spectra, IR spectra, Raman spectra were also computed in order to obtain the exact position of atoms present in title compound. The density of state (DOS) and its energies were also computed. Vibrational energy and contribution of each mode towards the potential energy of the molecule is reported.

2. Computational details

For meeting the requirements of both accuracy and computing economy, theoretical methods and basis sets should be considered. DFT has proved to be extremely useful in treating the electronic structure of molecules (Arivazhagan & Jeyavijayan 2011). Calculations were carried out theoretically with the help of Gaussian (Frisch et al. 2009) program package installed in Tyrone cluster of Super Computer Research Centre (SERC) of Indian Institute of Science (IISc), Bangalore, India. Gaussian software has various preinstalled exchange correlation functional. Becke’s three parameter hybrid functional with Lee–Yang–Parr correction (Lee et al. 1988) that is, B3LYP hybrid



functional (Becke et al. 1993) and LANL2DZ basis set (Dunning & Hay 1977, Hay & Wadt 1985) was used. The molecular structure of metanil yellow was drawn in GaussView 5.0.8 (Frisch et al. 2009) program and it is shown in Fig. 1. Geometrical optimization was performed by relaxing and converging the geometry of the molecule. This converged and optimized geometry corresponds to true minimum, as revealed by the lack of imaginary values in wavenumber calculations. The HOMO-LUMO molecular orbital levels, electrostatic potentials and Van der Waals surfaces were visualized using Avogadro program (Hanwel et al. 2012). The theoretical vibrational spectra and contribution of each mode towards potential energy were interpreted using VEDA 4 program (Jamroz 2004). Ultraviolet-visible spectrum and Density of State (DOS) diagram were obtained by using GaussSum program (O'Boyle et al. 2008). This program helps to calculate the contribution of group towards the molecular orbitals. The electronic population of each atom was determined and it contributed towards the determination of Mulliken atomic charges and atomic polar tensors (APT) (Ferreira 1993). The Gaussian program helps in getting the values of dipole moment, polarizability and first-order hyperpolarizability. These values were also obtained using DFT-B3LYP functional and LANL2DZ basis set. The final value of total polarizability and first-order hyperpolarizability were calculated theoretically using equations (1-3).

$$\mu = (\mu_x^2 + \mu_y^2 + \mu_z^2)^{1/2} \quad (1)$$

$$\alpha_{tot} = (\alpha_{xx} + \alpha_{yy} + \alpha_{zz}) / 3 \quad (2)$$

$$\beta_{tot} = [(\beta_{xxx} + \beta_{xyy} + \beta_{xzz})^2 + (\beta_{xyx} + \beta_{yyy} + \beta_{yzz})^2 + (\beta_{xxz} + \beta_{yyz} + \beta_{zzz})^2]^{1/2} \quad (3)$$

In closed shell Hartree-Fock theory, the negative of the HOMO energy represents ionization potential (I) (Koopmans & Tjalling 1934) and negative of LUMO represent electron affinity (A) (Zhang et al. 2007). The values of electronegativity (χ) (Parr et al. 1978, Parr & Pearson 1983), electrophilicity index (ω) (Parr et al. 1999), chemical potential (μ), hardness (η) (Pearson 2005), softness (S) etc. for metanil yellow can be calculated theoretically using equations (4-8).

$$\mu = -(I + A) / 2 \quad (4)$$

$$\chi = (I + A) / 2 \quad (5)$$

$$\eta = (I - A) / 2 \quad (6)$$

$$S = \eta / 2 \quad (7)$$

$$\omega = \mu^2 / 2\eta \quad (8)$$

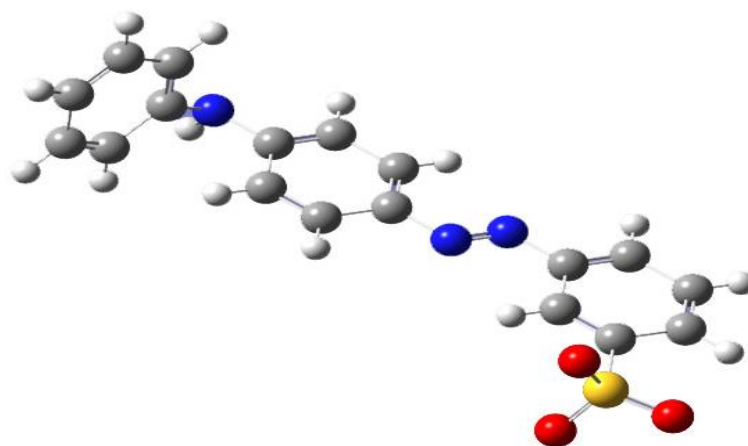


Fig. 1: Metanil Yellow.

3. Results and discussion

3.1. Geometrically optimized structure

The optimized molecular structure of metanil yellow along with numbering of each atom is shown in Fig. 2. DFT-B3LYP/ LANL2DZ method was used for obtaining the optimized geometry of metanil yellow. The optimized geometrical parameters of the title compound such as bond lengths, bond angles and dihedral angles are listed in Table 1. The other parameters of the title compound can be calculated from the calculated geometric parameters. The geometric optimized structure of metanil yellow reveals that the meta-substituted azo group is in planar with two benzene rings. The azo bond and SO₃ group which are known for their strong electron withdrawing nature, are expected to increase the contribution of the resonance structure. The electronic effect of azo bond contributes to increasing bond length of meta-substituted SO₃ group with C2-S11 bond length of 1.9016 Å. The bond length of azo bond that is, N15-N16 bond length is 1.292 Å and the dihedral angle of C4-N15-N16-C17 is found out to be -179.8752°. The C24-N27 and N27-C29 bond lengths are not the same. The ring carbon atoms in substituted benzenes exert a larger attraction on the valence electron cloud of the hydrogen atom resulting in an increase in the C-H force constants and a decrease in the corresponding bond length.

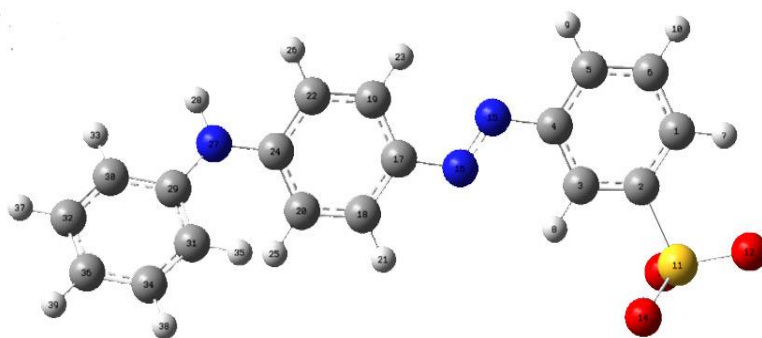


Fig. 2: Geometrically Optimized Structure of Metanil Yellow.

Table 1: Optimized Geometry of Metanil Yellow

Atoms	Bond Length (Å)	Atoms	Bond Angle(°)	Atoms	Dihedral Angle(°)
C1-C2	1.4047	C2-C1-C6	119.1324	C6-C1-C2-C3	-0.8694
C1-C6	1.4089	C2-C1-H7	118.4966	C6-C1-C2-S11	179.0886
C1-H7	1.0871	C6-C1-H7	122.3561	H7-C1-C2-C3	177.7577
C2-C3	1.3934	C1-C2-C3	122.1717	H7-C1-C2-S11	-2.2844
C2-S11	1.9016	C1-C2-S11	118.254	C2-C1-C6-C5	0.1498
C3-C4	1.4184	C3-C2-S11	119.5743	C2-C1-C6-H10	179.9558
C3-H8	1.0854	C2-C3-C4	118.4382	H7-C1-C6-C5	-178.4218
C4-C5	1.4145	C2-C3-H8	120.6398	H7-C1-6-H10	1.3843
C4-N15	1.4273	C4-C3-H8	120.9116	C1-C2-C3-C4	0.8995
C5-C6	1.4043	C3-C4-C5	120.1787	C1-C2-C3-H8	-177.9426
C5-H9	1.0872	C3-C4-N15	124.8249	S11-C2-C3-C4	-179.0579
C6-H10	1.0878	C5-C4-N15	114.9963	S11-C2-C3-H8	2.1
S11-O12	1.6504	C4-C5-C6	120.1609	C1-C2-S11-O12	25.4859
S11-O13	1.6465	C4-C5-H9	118.2443	C1-C2-S11-O13	-93.7428
S11-O14	1.6469	C6-C5-H9	121.5925	C1-C2-S11-O14	146.3822
N15-N16	1.292	C1-C6-C5	119.9106	C3-C2-S11-O12	-154.555
N16-C17	1.4279	C1-C6-H10	120.0281	C3-C2-S11-O13	86.2163
C17-C18	1.4114	C5-C6-H10	120.0611	C3-C2-S11-O14	-33.6587
C17-C19	1.4178	C2-S11-O12	102.2834	C2-C3-C4-C5	-0.2236
C18-C20	1.4019	C2-S11-O13	104.3134	C2-C3-C4-N15	179.8777
C18-H21	1.0865	C2-S11-O14	103.2755	H8-C3-C4-C5	178.6152
C19-C22	1.3964	O12-S11-O13	114.1867	H8-C3-C4-N15	-1.2835
C19-H23	1.0855	O12-S11-O14	116.07	C3-C4-C5-C6	-0.4652
C20-C24	1.4159	O13-S11-O14	114.3921	C3-C4-C5-H9	-179.9251
C20-H25	1.0844	C4-N15-N16	115.9768	N15-C4-C5-C6	179.443
C22-C24	1.4212	N15-N16-C17	115.118	N15-C4-C5-H9	-0.0168
C22-H26	1.0896	N16-C17-C18	115.8107	C3-C4-N15-N16	0.5149
C24-N27	1.4138	N16-C17-C19	125.283	C5-C4-N15-N16	-179.3885
N27-H28	1.0133	C18-C17-C19	118.9053	C4-C5-C6-C1	0.5005
N27-C29	1.4093	C17-C18-C20	121.1916	C4-C5-C6-H10	-179.3055
C29-C30	1.4193	C17-C18-H21	117.9434	H9-C5-C6-C1	179.9418
C29-C31	1.4179	C20-C18-H21	120.859	H9-C5-C6-H10	0.1358
C30-C32	1.4034	C17-C19-C22	120.0855	C4-N15-N16-C17	-179.8752
C30-H33	1.0892	C17-C19-H23	118.6556	N15-N16-C17-C18	179.9827
C31-C34	1.405	C22-C19-H23	121.256	N15-N16-C17-C19	0.3605
C31-H35	1.0843	C18-C20-C24	119.9985	N16-C17-C18-C20	-179.8695
C32-C36	1.4091	C18-C20-H25	119.6044	N16-C17-C18-H21	-0.7517
C32-H37	1.0881	C24-C20-H25	120.3611	C19-C17-C18-C20	-0.2219
C34-C36	1.4085	C19-C22-C24	121.0799	C19-C17-C18-H21	178.8959
C34-H38	1.088	C19-C22-H26	119.8737	N16-C17-C19-C22	-179.6555
C36-H39	1.0868	C24-C22-H26	119.0432	N16-C17-C19-H23	-0.2614
		C20-C24-C22	118.7327	C18-C17-C19-C22	0.7331
		C20-C24-N27	123.256	C18-C17-C19-H23	-179.8729
		C22-C24-N27	117.9475	C17-C18-C20-C24	-0.5144
		C24-N27-H28	115.1051	C17-C18-C20-H25	177.311
		A(24-N27-C29)	129.583	H21-C18-C20-C24	-179.6065
		H28-N27-C29	115.307	H21-C18-C20-H25	-1.7812
		N27-C29-C30	118.213	C17-C19-C22-C24	-0.5147
		N27-C29-C31	123.151	C17-C19-C22-H26	178.8285
		C30-C29-C31	118.5791	H23-C19-C22-C24	-179.8927
		C29-C30-C32	120.7397	H23-C19-C22-H26	-0.5495
		C29-C30-H33	119.3194	C18-C20-C24-C22	0.7307
		C32-C30-H33	119.9384	C18-C20-C24-N27	177.7619
		C29-C31-C34	120.1231	H25-C20-C24-C22	-177.0779
		C29-C31-H35	120.1601	H25-C20-C24-N27	-0.0468
		C34-C31-H35	119.6884	C19-C22-C24-C20	-0.2209
		C30-C32-C36	120.5653	C19-C22-C24-N27	-177.4106
		C30-C32-H37	119.369	H26-C22-C24-C20	-179.5694
		C36-C32-H37	120.063	H26-C22-C24-N27	3.2408
		C31-C34-C36	121.1611	C20-C24-N27-H28	-154.75
		C31-C34-H38	118.9344	C20-C24-N27-C29	26.0976
		C36-C34-H38	119.9006	C22-C24-N27-H28	22.303

C32-C36-C34	118.826	C22-C24-N27-C29	-156.8494
C32-C36-H39	120.5864	C24-N27-C29-C30	-160.7787
C34-C36-H39	120.5874	C24-N27-C29-C31	22.0082
		H28-N27-C29-C30	20.0703
		H28-N27-C29-C31	-157.1428
		N27-C29-C30-C32	-177.3846
		N27-C29-C30-H33	3.1937
		C31-C29-C30-C32	-0.0415
		C31-C29-C30-H33	-179.4632
		N27-C29-C31-C34	177.8009
		N27-C29-C31-H35	-0.2537
		C30-C29-C31-C34	0.5974
		C30-C29-C31-H35	-177.4572
		C29-C30-C32-C36	-0.6242
		C29-C30-C32-H37	179.9793
		H33-C30-C32-C36	178.7939
		H33-C30-C32-H37	-0.6026
		C29-C31-C34-C36	-0.5022
		C29-C31-C34-H38	-179.7868
		H35-C31-C34-C36	177.5616
		H35-C31-C34-H38	-1.723
		C30-C32-C36-C34	0.7209
		C30-C32-C36-H39	-179.4483
		H37-C32-C36-C34	-179.8868
		H37-C32-C36-H39	-0.056
		C31-C34-C36-C32	-0.16
		C31-C34-C36-H39	-179.9908
		H38-C34-C36-C32	179.1178
		H38-C34-C36-H39	-0.713

3.2. Molecular orbital analysis

The electronic absorption corresponds to the transition from the ground to the first excited state and is mainly described by one electron excitation from the highest occupied molecular orbital (HOMO) to the lowest unoccupied molecular orbital (LUMO). The DFT-B3LYP/LANL2DZ method was used in order to compute HOMO-LUMO energy gap of metanil yellow. HOMO (Fig. 3.1) and LUMO (Fig. 3.2) which represent the plot of electron density for particular molecule are represented in Fig. 3. The band gap value found out to be 2.17 eV with HOMO energy of -2.4 eV and LUMO energy of -0.23 eV from the used exchange correlation functional. The LUMO has an electron acceptor represents the ability to obtain an electron, and HOMO represents the ability to donate an electron. The small value of band gap witnesses the chemical activity of the compound. This also proves the considerable application of metanil yellow as nonlinear optical material.

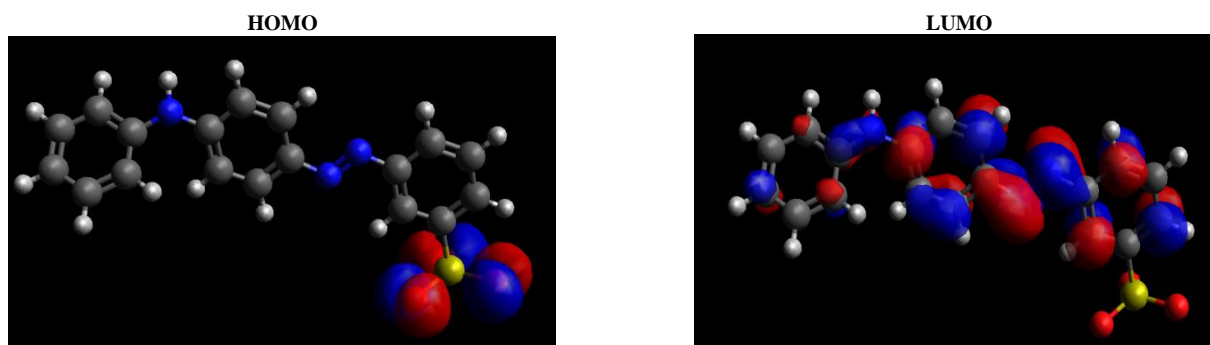


Fig. 3: HOMO-LUMO.

3.3. Van der Waals forces

The DFT-B3LYP/LANL2DZ method was used in order to analyse Van der Waals field. This analysis was performed using Avogadro software and the surfaces are shown in Fig. 4.

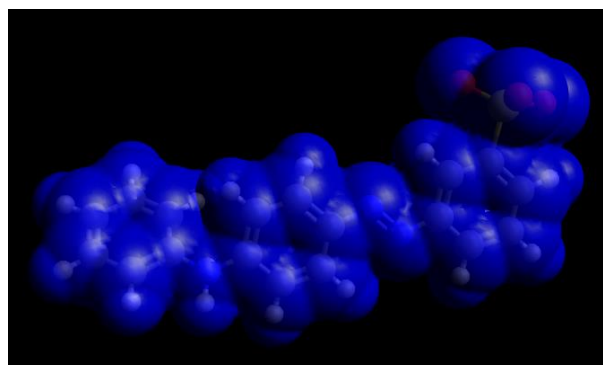


Fig. 4: Van der Waals Forces.

3.4. Nonlinear optical properties

The Dipole moment μ (D), polarizability and first-order hyperpolarizability of metanil yellow helped us to study nonlinear optical properties (NLO). The dipole moment of the title compound was found out to be 29.1368 D. The polarizability and first order hyperpolarizability values of metanil yellow are calculated using equations (2, 3) and found out to be -216.7941 a.u. and 1330.0961 a.u. respectively. These properties were obtained using DFT-B3LYP method and LANL2DZ basis set. The considerably high value of dipole moment and hyperpolarizability of the title compound is the proof for the compound to have large NLO optical property. Dipole moment, polarizability and hyperpolarizability of the title compound are summarized in Table 2.

Table 2: Electric Dipole Moment M (D), Polarizability A_{tot} ($\times 10^{-23}$ Esu) and First Order Hyperpolarizability B_{tot} ($\times 10^{-23}$ Esu) Values

Parameter	Value	Parameter	Value
μ_x	-27.1971	β_{xxx}	-1084.7911
μ_y	10.4173	β_{xxy}	374.42
μ_z	0.8644	β_{xyy}	-127.3888
μ (D)	29.1368	β_{yyy}	61.4033
α_{xx}	-316.1288	β_{xxz}	0.4295
α_{xy}	53.3461	β_{xyz}	24.3903
α_{yy}	-165.1084	β_{yyz}	6.9892
α_{xz}	10.5545	β_{xzz}	-41.7747
α_{yz}	-4.1306	β_{yzz}	7.3467
α_{zz}	-169.1452	β_{zzz}	11.394
α_{tot} (a.u)	-216.7941	β_{tot} (a.u)	1330.0961

3.5. Vibrational assignments

The evidence for the charge transfer interaction between the donor and acceptor groups through π -electron movement is provided by the vibrational spectral studies. Metanil yellow consists of 39 atoms and 174 electrons. It is a negatively charged compound with a single multiplicity. Atoms of the title compound have 111 normal modes of vibration. The potential energy distribution (PED) and the contribution of atomic stretches towards Raman frequencies are obtained using VEDA program. Output of VEDA is used in order to get vibrational assignments of the title compound. Table 3 summarizes vibrational frequency assignments of metanil yellow.

The infrared spectra and bulk Raman spectra for metanil yellow are obtained and shown in Fig. 5 and 6 respectively. The CH_3 stretching is usually found to have a frequency of 3000 cm^{-1} (Silverstein et al. 1981). The title compound shows the peak for CH_3 stretching at the frequency of 3241 cm^{-1} which is contributed by 99% of stretching potential energy. Potential energy distribution using VEDA software is useful for calculating the contribution of stretching potential energy towards the frequency. Similarly the stretch of N-H, N=N, N-C, S-O bond has frequency of 3625, 1431, 1258, 898 cm^{-1} respectively. The C-C bond stretch for aromatic compounds shows the frequency within range 1100 to 1650 cm^{-1} (Roeges 1994, Clothup et al. 1990). Contribution of each stretch and bends towards Raman frequency is shown in Table 3. For example, consider N-C stretch (s34) for N (atom number 16) and C (atom number 17) – 23% of the stretching potential energy contributes to 1258 cm^{-1} vibration and 15% contributes to 1172 cm^{-1} vibration. Similarly, the atomic stretches contributing to vibration can be determined. For example, the atomic stretches contributing to 1258 cm^{-1} can be obtained by comparing stretches of s33, s34, s44 and s50. Thus, atomic stretches contributing to 1258 cm^{-1} vibration are N16-C17, N15-C4, H8-C3-C2 and H26-C22-C19 in decreasing order of contribution. Also, STRE, BEND, TORS and OUT represents stretching, bending, torsional and out of plane modes respectively.

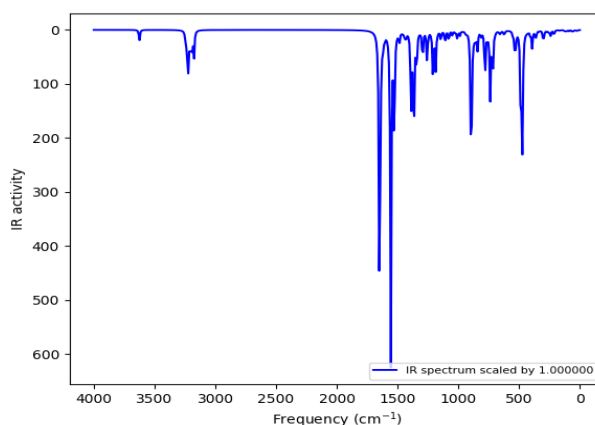


Fig. 5: IR Spectra.

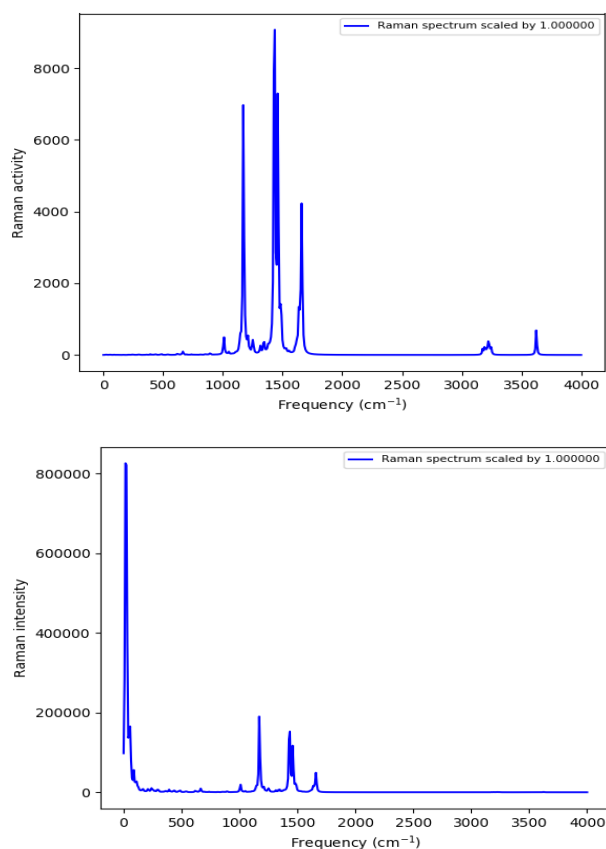


Fig. 6: Raman Spectra.

Table 3: Potential Energy Distribution (PED)

Average max. Potential Energy <EPm> = 31.019							
TED Above 100 Factor TAF=0.000							
Average coordinate population 1.000							
s1	STRE	27	28	NH	1.013264	f3625 100	
s2	STRE	1	4	CH	1.087059	f3227 48 f3216 42	
s3	STRE	3	8	CH	1.085399	f3241 99	
s4	STRE	5	9	CH	1.087188	f3227 26 f3216 55 f3191 19	
s5	STRE	6	10	CH	1.087791	f3227 25 f3191 72	
s6	STRE	18	21	CH	1.086548	f3240 20 f3219 67	
s7	STRE	19	23	CH	1.085513	f3236 91	
s8	STRE	20	25	CH	1.084430	f3247 31 f3240 36 f3219 29	
s9	STRE	22	26	CH	1.089591	f3175 92	
s10	STRE	30	33	CH	1.089238	f3203 16 f3192 11 f3176 66	
s11	STRE	31	35	CH	1.084298	f3247 54 f3240 30	
s12	STRE	32	37	CH	1.088067	f3225 21 f3203 46 f3176 25	
s13	STRE	34	38	CH	1.087963	f3203 30 f3192 50	
s14	STRE	36	39	CH	1.086844	f3225 55 f3192 31	
s15	STRE	3	2	CC	1.393437	f1637 21 f1391 14	
s16	STRE	16	15	NN	1.292014	f1461 36 f1431 43	
s17	STRE	22	19	CC	1.396432	f1661 16 f1648 14 f1445 15	
s18	STRE	2	1	CC	1.404736	f1637 10 f1488 12 f1391 14 f1109 12 f1079 12	
s19	STRE	6	5	CC	1.404275	f1637 14 f1391 14 f1109 17	
s20	STRE	20	18	CC	1.401879	f1445 13	
s21	STRE	30	32	CC	1.403447	f1661 15 f1648 15 f1112 14	
s22	STRE	1	6	CC	1.408939	f1608 35 f1187 11 f1079 18 f1008 10	
s23	STRE	34	31	CC	1.404998	f1112 13	
s24	STRE	32	36	CC	1.409143	f1112 10 f1049 26	
s25	STRE	36	34	CC	1.408547	f1638 15 f1049 21	
s26	STRE	4	5	CC	1.414483	f1637 20 f1608 10 f1488 10 f1391 16	
s27	STRE	18	17	CC	1.411428	f1648 11 f1622 16	
s28	STRE	19	17	CC	1.417783	f1380 11	
s29	STRE	24	20	CC	1.415883	f1622 23 f1380 17 f1294 11	
s30	STRE	31	29	CC	1.417860	f1638 16 f1380 10 f1294 10	
s31	STRE	27	29	NC	1.409294	f1366 16 f1248 15	
s32	STRE	27	24	NC	1.413809	f1555 10 f1248 19	
s33	STRE	15	4	NC	1.427274	f1258 12 f1209 15	
s34	STRE	16	17	NC	1.427910	f1258 23 f1172 15	
s35	STRE	11	13	SO	1.646539	f898 23 f893 40 f738 22	
s36	STRE	11	14	SO	1.646919	f898 59 f738 23	
s37	STRE	11	12	SO	1.650425	f893 47 f738 25	
s38	STRE	11	2	SC	1.901641	f253 10 f240 36	
s39	BEND	22	19	17	CCC	120.09	f1025 38 f655 14

s40	BEND	30	32	36	CCC	120.57	f1009 28 f633 25	
s41	BEND	4	5	6	CCC	120.16	f1608 10 f535 18	
s42	BEND	28	27	29	HNC	115.31	f1638 17 f1555 31 f1528 12 f1294 15	
s43	BEND	7	1	6	HCC	122.36	f1488 12 f1314 13 f1187 15 f1109 18	
s44	BEND	8	3	2	HCC	120.64	f1488 14 f1314 29 f1258 11 f1079 17	
s45	BEND	9	5	3	HCC	121.59	f1314 17 f1187 14 f1109 15	
s46	BEND	10	6	1	HCC	120.03	f1488 26 f1314 15 f1187 30	
s47	BEND	21	18	20	HCC	120.86	f1343 28 f1172 17 f1144 10	
s48	BEND	23	19	22	HCC	121.26	f1343 10 f1209 11 f1144 27	
s49	BEND	25	20	24	HCC	120.36	f1343 21	
s50	BEND	26	22	19	HCC	119.87	f1529 11 f1343 10 f1258 11 f1209 10 f1144 13	
s51	BEND	33	30	32	HCC	119.94	f1528 12 f1388 12 f1223 19 f1112 10	
s52	BEND	35	31	34	HCC	119.69	f1366 25 f1223 22 f1112 10	
s53	BEND	37	32	36	HCC	120.06	f1223 12 f1202 28	
s54	BEND	38	34	36	HCC	119.90	f1366 12 f1223 23 f1202 17	
s55	BEND	39	36	34	HCC	120.59	f1485 11 f1202 34 f1112 16	
s56	BEND	3	2	1	CCC	122.17	f1608 11 f1079 11 f1008 32 f667 11	
s57	BEND	16	15	4	NCC	115.98	f942 12 f535 10 f165 11 f53 10 f28 20	
s58	BEND	2	1	6	CCC	119.13	f1008 17 f942 18	
s59	BEND	20	18	17	CCC	121.19	f1025 23 f655 27	
s60	BEND	1	6	5	CCC	119.91	f1008 18 f667 19	
s61	BEND	34	31	29	CCC	120.12	f633 17	
s62	BEND	32	36	34	CCC	118.83	f1009 16 f890 13	
s63	BEND	36	34	31	CCC	121.16	f1009 15 f633 35	
s64	BEND	18	17	16	CCN	115.81	f545 11	
s65	BEND	19	17	16	CCN	125.28		
s66	BEND	24	20	18	CCC	120.00	f655 18	
s67	BEND	31	29	27	CCN	123.15	f357 17	
s68	BEND	29	27	24	CNC	129.58	f125 11 f28 11	
s69	BEND	27	24	20	NCC	123.26	f335 12 f28 10	
s70	BEND	15	4	5	NCC	115.00	f535 17 f53 10 f28 11	
s71	BEND	17	16	15	CNN	115.12	f942 13 f535 11 f108 10 f28 16	
s72	BEND	13	11	12	OSO	114.19	f475 18 f365 11 f335 11 f301 17 f240 16	
s73	BEND	14	11	16	OSO	114.39	f475 22 f365 16 f301 16 f270 16	
s74	BEND	12	11	14	OSO	116.07	f475 14 f365 16 f253 43	
s75	BEND	11	2	1	SCC	118.25	f407 17 f165 17 f108 14 f89 10	
s76	TORS	28	27	29	HNCC	-20.07	f527 18 f486 39 f472 12 f392 11	
s77	TORS	7	1	2	11	HCCS	2.28	f1028 37 f966 25 f842 15
s78	TORS	8	3	2	11	HCCS	-2.10	f987 55 f966 27
s79	TORS	9	5	6	1	HCCC	-179.94	f1028 11 f987 20 f966 24 f842 16 f716 14
s80	TORS	10	6	1	2	HCCC	-179.96	f1028 34 f842 48
s81	TORS	21	18	20	24	HCCC	-180.39	f1031 13 f1015 18 f888 15
s82	TORS	23	19	22	24	HCCC	-180.11	f1023 36 f1015 14 f870 14
s83	TORS	25	20	24	27	HCCN	0.05	f1031 14 f1015 13 f888 30
s84	TORS	26	22	24	27	HCCN	-3.24	f1023 17 f888 11 f870 34 f858 14
s85	TORS	33	30	32	36	HCCC	-178.79	f1004 10 f934 21 f870 15 f719 11 f424 11
s86	TORS	35	31	34	36	HCCC	-177.56	f1031 12 f1004 10 f934 29 f870 10 f424 10
s87	TORS	37	32	36	34	HCCC	-180.11	f1004 34 f780 15
s88	TORS	38	34	36	32	HCCC	-179.12	f1031 24 f1004 15 f780 12
s89	TORS	39	36	34	31	HCCC	-180.01	f934 28 f780 19 f719 12
s90	TORS	3	2	1	4	CCCC	0.87	f966 10 f716 13 f365 10 f292 13 f253 12
s91	TORS	16	15	4	3	NNCC	-0.51	f292 11 f125 18 f18 32
s92	TORS	22	19	17	18	CCCC	-0.73	f759 17 f551 10 f437 15 f392 17
s93	TORS	2	1	6	5	CCCC	-0.15	f716 15 f292 30
s94	TORS	20	18	17	16	CCCN	-180.13	f437 32 f24 11
s95	TORS	30	32	36	34	CCCC	-0.72	f719 15 f424 36
s96	TORS	34	31	29	27	CCCN	-177.80	f213 29 f210 15
s97	TORS	32	36	34	31	CCCC	0.16	f719 11 f486 16 f424 23
s98	TORS	36	34	31	29	CCCC	0.50	f780 22 f719 27
s99	TORS	4	5	6	1	CCCC	-0.50	f716 26 f472 15
s100	TORS	18	17	16	15	CCNN	-179.98	f210 14 f125 14 f61 11 f18 33
s101	TORS	24	20	18	17	CCCC	0.51	f759 38
s102	TORS	31	29	27	24	CCNC	-22.01	f125 10 f53 34 f28 10 f24 11
s103	TORS	29	27	24	20	CNCC	-26.10	f89 15 f61 31 f24 17
s104	TORS	27	24	20	18	NCCC	-177.76	f551 12 f392 12 f210 13 f24 18
s105	TORS	17	16	15	4	CNNC	-180.12	f61 13 f24 17
s106	TORS	12	11	2	3	OSCC	-205.44	f13 84
s107	OUT	14	2	13	11	OCOS	57.56	f407 45 f165 20
s108	OUT	13	2	12	11	OCOS	57.74	f365 26 f114 21
s109	OUT	11	3	1	2	SCCC	0.04	f624 11 f617 13 f114 22 f108 15
s110	OUT	19	18	16	17	CCNC	0.31	f759 12 f551 26
s111	OUT	15	3	5	4	NCCC	0.08	f624 13 f617 17

3.6. Global chemical reactivity parameters and thermodynamic parameters

The energy values of HOMO and LUMO are useful in calculating ionization potential, electron affinity of the title compound. The HOMO and LUMO energies were obtained from DFT calculations using B3LYP exchange correlation hybrid functional and LANL2DZ basis set. The values of electronegativity, electrophilicity index, chemical potential, etc. for metanil yellow can be calculated theoretically. These values of global chemical reactivity descriptors of compounds are listed in Table 4. Ionization potential and electron affinity of

the title compound are 2.4 and 0.23 respectively. Other general chemical reactivity parameters were also obtained from these values. The thermochemistry and thermodynamic parameters are also listed in Table 5. The negative value of the chemical potential is fair enough for proving that the title compound is thermodynamically stable.

Table 4: Global Reactivity Parameters

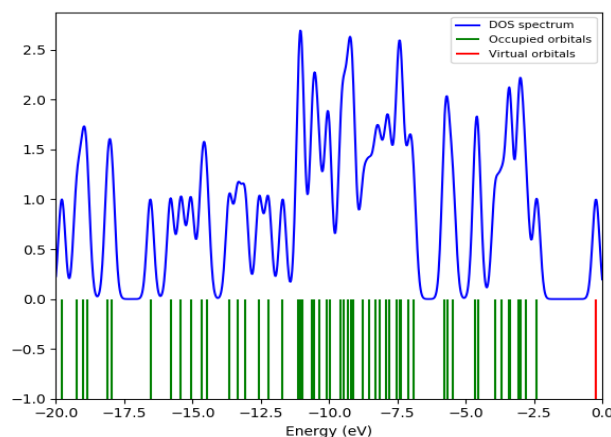
Parameter	Value	Parameter	Value
$\mu(D)$	29.1368	I	2.4
α_{tot} (a.u)	-216.7941	A	0.23
β_{tot} (a.u)	1330.0961	μ	-1.315
HOMO (eV)	-2.4	χ	1.315
LUMO (eV)	-0.23	η	1.085
ΔE (eV)	2.17	S	0.5425
		ω	0.7969

Table 5: Thermodynamic Parameters

Zero-point correction (Hartree/Particle)	0.289055
Thermal correction to Energy	0.310416
Thermal correction to Enthalpy	0.311361
Thermal correction to Gibbs Free Energy	0.234368
Sum of electronic and zero-point Energies	-1093.762182
Sum of electronic and thermal Energies	-1093.740821
Sum of electronic and thermal Enthalpies	-1093.739877
Sum of electronic and thermal Free Energies	-1093.816869

3.7. UV-Vis spectra and density of states

The UV-Vis spectra and DOS were obtained from DFT calculations using B3LYP exchange correlation hybrid functional and LANL2DZ basis set. GaussSum software was used to plot the UV-Vis spectra and Density of state spectrum shown in Fig. 7. The bandgap obtained from the energies of frontier molecular orbitals is represented in Table 4. This bandgap is compared with the energy gap obtained from the UV-Vis spectra and found out to be equal in value.

**Fig. 7:** UV-Vis Spectra and DOS.

3.8. Atomic charges and population analysis

Obtained Mulliken charges and atomic tensors for each atom is listed in Table 6. The maximum atomic charge is obtained for S11 when compared with other atoms. This is due to the attachment of negatively charged carbon O12, O13 and O14 atoms.

Table 6: Atomic Charges and Population Analysis

atoms	Mulliken	APT	atoms	Mulliken	APT	atoms	Mulliken	APT
C1	-0.224792	-0.103019	O14	-0.6676	-0.7461	N27	-0.51547	-1.30619
C2	-0.062626	-0.270089	N15	-0.13209	0.169405	H28	0.286834	0.163811
C3	-0.274698	-0.084429	N16	-0.09993	0.045425	C29	0.438544	0.82866
C4	0.181457	-0.19144	C17	0.153932	-0.14387	C30	-0.43434	-0.30039
C5	-0.350928	0.021293	C18	-0.34374	0.113855	C31	-0.37048	-0.21176
C6	-0.18816	-0.101795	C19	-0.27424	0.066879	C32	-0.18862	0.103062
H7	0.281979	0.113096	C20	-0.36174	-0.24584	H33	0.214447	0.042853
H8	0.309696	0.128211	H21	0.254422	0.077315	C34	-0.20785	0.116079
H9	0.227195	0.058984	C22	-0.41995	-0.3414	H35	0.261242	0.069169
H10	0.210963	-0.008475	H23	0.266749	0.088918	C36	-0.25953	-0.23727
S11	1.072248	1.641824	C24	0.456171	0.887487	H37	0.211231	0.013577
O12	-0.675525	-0.800213	H25	0.252463	0.045143	H38	0.216441	0.031445
O13	-0.671589	-0.773228	H26	0.211628	0.013137	H39	0.216232	0.025865

4. Conclusion

In this work, detail quantum chemical study of metanil yellow was done. Density Functional Theory (DFT) was used in analysing the geometrical optimization of metanil yellow using B3LYP exchange correlation functional and LANL2DZ basis set in order to obtain

bond lengths and bond angles. The Vibrational analysis consisting of Vibrational wavenumbers, Raman intensities, vibrational frequencies, IR intensities and force constant were computed. DFT was used in order to calculate dipole moment, polarizability and first-order hyperpolarizability of the studied compound. The total surface analysis along with potential energy distribution was also studied for the titled compound. The density of state analysis was done in order to obtain the energy contribution of each electron. HOMO-LUMO orbital energies were calculated and lowering of HOMO-LUMO energy gap explains the charge transfer interactions taking place within the molecule. These HOMO-LUMO energies can be used for obtaining some molecular properties such as electron affinity, ionization potential, chemical potential, etc. of the title compound. In the end, all these results showed that the title compound exhibits considerable NLO properties.

References

- [1] Dhakal S, Chao K, Schmidt W, Qin J, Kim M & Chan D (2016), Evaluation of Turmeric Powder Adulterated with Metanil Yellow using FT-Raman and FT-IR Spectroscopy. *Foods* 5 (2), 36. DOI: <https://doi.org/10.3390/foods5020036>.
- [2] "Common food adulterants in India", *India Today*, New Delhi, October 19, 2018. Available at: <https://www.indiatoday.in/education-today/gk-current-affairs/story-common-food-adulterants-in-india-1370601-2018-10-19>.
- [3] Nath PP, Sarkar K, Mondal M & Paul G. (2016), Metanil yellow impairs the estrous cycle physiology and ovarian folliculogenesis in female rats. *Environ Toxicol* 31, 2057-67. <https://doi.org/10.1002/tox.22205>.
- [4] Ghosh D, Singha PS, Firdaus SB & Ghosh S, (2017), Metanil yellow: The toxic food colorant 4(4), 65-66. <https://doi.org/10.21276/apjhs>.
- [5] Hazra S, Dome RN, Ghosh S & Ghosh D. (2016), Protective effect of methanolic leaves extract of *Coriandrum sativum* against metanil yellow induced lipid peroxidation in goat liver: An in vitro study. *Int J Pharmacol Pharma Sci*, 3(5), 34-41.
- [6] Sarkar R. (2013), Histopathological changes in the brain of metanil yellow treated albino rat (*Rattus norvegicus*). *Int J Basic App Med Sci* 2013; 3:256-8.
- [7] Das M, Ramchandani S, Upreti RK & Khanna SK (1997), Metanil Yellow: a Bifunctional Inducer of Hepatic Phase I and Phase II Xenobiotic Metabolizing Enzymes. *Food and Chemical Toxicology* 35 (8), 835-838. [https://doi.org/10.1016/S0278-6915\(97\)00047-1](https://doi.org/10.1016/S0278-6915(97)00047-1).
- [8] Frisch MJ, et al., (2009), Gaussian 09, Revision B.01, Gaussian Inc., Wallingford CT.
- [9] Lee C, Yang W & Parr RG (1988), Development of the Colle-Salvetti correlation energy formula into a functional of the electron density. *Physical Review B* 37 (2), 785-789. <https://doi.org/10.1103/PhysRevB.37.785>.
- [10] Arivazhagan M & Jeyavijayan S (2011), Vibrational spectroscopic, first-order hyperpolarizability and HOMO, LUMO studies of 1, 2-dichloro-4 nitrobenzene based on Hartree-Fock and DFT calculations. *Spectrochimica Acta Part A: Molecular and Biomolecular Spectroscopy* 79 (2), 376-383. <https://doi.org/10.1016/j.saa.2011.03.036>.
- [11] Becke AD (1993), Density-functional thermochemistry. III. The role of exact exchange. *The Journal of Chemical Physics* 98(7), 5648-5652. DOI: <https://doi.org/10.1063/1.464913>.
- [12] Dunning TH Jr. & Hay PJ (1977), In: "Modern Theoretical Chemistry", Ed H F. Schaefer III, Vol. 3 (Plenum, New York, 1977) 1-28.
- [13] Hay PJ & Wadt WR (1985), Ab initio effective core potentials for molecular calculations – potentials for the transition-metal atoms Sc to Hg. *J. Chem. Phys.*, 82, 270-83. <https://doi.org/10.1063/1.448799>.
- [14] Frisch E, Hratchian HP, Dennington II RD, Keith TA, Millam J, Nielsen B, Holder AJ & Hiscocks J (2009), Gaussian, Inc. GaussView Version 5.0.8, Wallingford, CT.
- [15] Hanwell MD, Curtis DE, Lonie DC, Vandermeersch T, Zurek E & Hutchison GR (2012), Avogadro: an advanced semantic chemical editor, visualization, and analysis platform. *Journal of Cheminformatics* volume 4, Article number: 17. <https://doi.org/10.1186/1758-2946-4-17>.
- [16] Jamroz MH (2004), Vibrational Energy Distribution Analysis: VE-DA 4 Program. Warsaw, Poland.
- [17] O'Boyle NM, Tenderholt AL & Langner KM (2008), cclib: A library for package-independent computational chemistry algorithms. *J. Comp. Chem.* 29, 839-845. <https://doi.org/10.1002/jcc.20823>.
- [18] Ferreira MMC (1993), Population analysis from atomic polar tensors. *Journal of Molecular Structure* 294, 75-78. DOI: [https://doi.org/10.1016/0022-2860\(93\)80318-P](https://doi.org/10.1016/0022-2860(93)80318-P).
- [19] Koopmans & Tjalling (1934), Über die Zuordnung von Wellenfunktionen und Eigenwerten zu den einzelnen Elektronen eines Atoms. *Physica*. 1 (1-6), 104- 113. [https://doi.org/10.1016/S0031-8914\(34\)90011-2](https://doi.org/10.1016/S0031-8914(34)90011-2).
- [20] Zhang, Gang, Musgrave & Charles B. (2007), Comparison of DFT Methods for Molecular Orbital Eigenvalue Calculations. *The Journal of Physical Chemistry A* 111 (8), 1554-1561. <https://doi.org/10.1021/jp061633o>.
- [21] Parr RG, Donnelly RA, Levy M & Palke WE (1978), Electronegativity: the density functional viewpoint. *Journal of Chemical Physics* 68(8), 3801-3807. <https://doi.org/10.1063/1.436185>.
- [22] Parr RG & Pearson RG (1983), Absolute hardness: companion parameter to absolute electronegativity. *Journal of the American Chemical Society* 105(26), 7512-7516. <https://doi.org/10.1021/ja00364a005>.
- [23] Parr RG, Szentpály LV & Liu S (1999) Electrophilicity Index. *Journal of the American Chemical Society* 121(9), 1922-1924. DOI: <https://doi.org/10.1021/ja983494x>.
- [24] Pearson RG (2005) Chemical hardness and density functional theory. *Journal of Chemical Sciences* 117(5), 369-377. DOI: <https://doi.org/10.1007/BF02708340>.
- [25] Silverstein RM, Basseler GC & Morill C (1981) *Spectrometric Identification of Organic Compounds*, Wiley, New York. DOI: <https://doi.org/10.1002/oms.1210260923>.
- [26] Roeges NPG (1994) *A Guide to the Complete Interpretation of IR Spectra of Organic Compounds*, Wiley, New York.
- [27] Clothup NB, Daly LH & Wiberly SE (1990) *Introduction to IR and Raman Spectroscopy*, Academic Press, New York.